

## NEW TRANSIENT FAULT LOCATION METHOD IN NON-SOLIDLY EARTHED SYSTEM FOR DISTRIBUTION NETWORK

Tianyou LI

State Grid Fujian Electric Power Co, Ltd – China  
2986010898@qq.com

Chaoyi Huang

State Grid Quanzhou Power Supply Company – China  
165480413@qq.com

### **ABSTRACT**

The technology of faulted line detection for non-solidly earthed distribution network has a wide range of applications in China and it has made significant achievements. However, the accuracy of the faulted section location (FSL) technique is not very high, which affects its large scale application. Therefore, the focus of this paper is to analyze the limitations of the existing techniques and to give some practical improvements. The paper establishes a trial network in Xiamen, Fujian Province, China to comprehensively demonstrate the practicality of the new technique. The results show that the system can achieve accurate faulted section location and will be promoted for large-scale application.

### **0 INTRODUCTION**

Compared with the transmission network, there is a high occurrence of earth faults in the medium-voltage distribution network, bringing undesired troubles to many power supply utilities. To improve power supply reliability and customers' satisfaction, China has recently expanded the investment in distribution network transformation. However, single-phase earth fault (SPEF) detection technology is still limited by the measuring principle, device design, network structure, etc. Its function in the existing distribution automation system (DAS) is relatively weak. Moreover, the accuracy of faulted section location system implemented by the feeder terminal units (FTUs) and the fault passage indicators etc. is generally low.

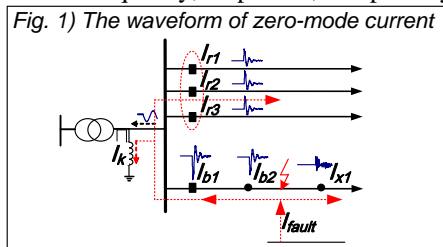
In recent years, the application of waveform correlation analysis for FSL method becomes very popular. The application often ignores the effective trade-offs between polarity, amplitude, noise and other factors, resulting in low accuracy in the field. The location method has to be supplemented by the traditional manual technique, which consumes a large amount of manpower and material resources. Improving the computational techniques of faulted section location so as to provide a comprehensive overall SPEF location scheme through SCADA or DA (Distribution Automation) system has become an urgent task [1-3].

### **1 THE TRADITIONAL FSL METHOD OF WAVEFORM COMPARISON**

#### **1.1 FSL Principle**

The transient current characteristics on both sides of the faulted section are determined by the different parameters of their equivalent zero mode networks, and they have

opposite polarities. Therefore, the characteristics of the zero mode currents can be effectively applied in FSL technique. The transient zero mode current upstream from the fault is the sum of the distributed capacitive currents for all the non-faulted lines and all the sections upstream from the measuring point. Its characteristics are high amplitude, low frequency, and the direction of current is from the fault point to the bus. The transient zero mode current downstream from the fault is the sum of the distributed capacitive current for all the rest of the downstream sections. Its characteristics are low amplitude, high frequency, and the direction of current is from fault point to the end of the line. As shown in figure 1, the characteristics of the transient current waveforms on both sides of the faulted section can be applied to perform faulted section location. These characteristics include frequency, amplitude, and polarity relationship [4].



#### **1.2 FSL Scheme**

The correlation coefficient reflecting the relationship between different amplitudes and phases is widely used in feature extraction for the digit signal processing. Therefore, the correlation coefficient can be used by the correlation analysis of zero-module transient current at each measuring point on the feeder. This method is called "included angle cosine" method as follows [5].

$$\rho_{m,n} = \frac{\sum_{m=1}^N i_{0,m}(m) \sum_{n=1}^N i_{0,n}(n)}{\sqrt{\sum_{m=1}^N i_{0,m}^2(m) \sum_{n=1}^N i_{0,n}^2(n)}} \quad (1)$$

Where  $i_{0,m}(k)$ 、 $i_{0,n}(k)$  is related with the different period of zero-module current on their corresponding terminal.

TAB.1 Correspondence between correlation coefficient

No.	Range	Distinguish
1	$\rho_{m,n} > 0$	Positive correlation; else negative.
2	$\rho_{m,n} = 0$	No association
3	$0 <  \rho_{m,n}  > 1$	Have association, the greater the coefficient, the greater the correlation

Therefore, this method sets a threshold  $\delta$ . When the correlation coefficients of the zero mode transient current in #m FTU and #n FTU meet the following formula, the fault is judged to occur between these two FTUs. Otherwise the fault is outside this section. Experience suggests that  $\delta$  ranges from 0.5 to 0.7.

$$|\rho_{m,n}| < \delta \quad (2)$$

### 1.3 Localization Limitation

The faulted section location criterion based on Eq. 2 does not require voltage signals. It only requires zero mode currents. Therefore, it is simple to implement. It also has big margin and good flexibility. However, there are some limitations.

#### 1.3.1 Strongly coupled zero mode currents on either side of the faulted section cannot be discriminated

Under some special circumstances, the line to ground capacitive currents upstream and downstream of the faulted section cannot be distinguished. These situations occur when there are large cable sections in the downstream route. In this case, strong coupling will appear and the following may occur.

$$-1 \leq \rho_{m,n} \leq -\delta \quad (3)$$

This corresponds to  $|\rho_{m,n}| > \delta$  for the faulted section. Therefore, the system fails to locate the faulted section and may even misjudge the fault to occur at the end of the line.

Thus, if the method does not consider the influence of polarity, it can have blind areas and can misjudge the faulted section.

#### 1.3.2 Accurate location is affected by zero drift value and noise jamming

Due to electromagnetic interference, the aging of equipment, etc, the waveforms acquired by the CT may be contaminated by noise and zero drift. Eq. 1 fails to consider the above factors, and may lead to failures when interference occurs<sup>[6]</sup>.

#### 1.3.3 It ignores the influence of amplitude on the correlation coefficient

Eq. 1 only reflects the extent of the relationship between signals, it does not quantify the difference of the signal amplitudes. However, the difference in amplitudes on the both sides of fault location is obvious. Thus, the influence of current amplitude needs to be considered. For instance, two signals may have the same frequency and phase signal but with different varying amplitudes, the correlation coefficients are all equal to 1. This is demonstrated with  $y = A \cos(2\pi 50t + 30)$ , changing the value of A does not change the correlation coefficient.

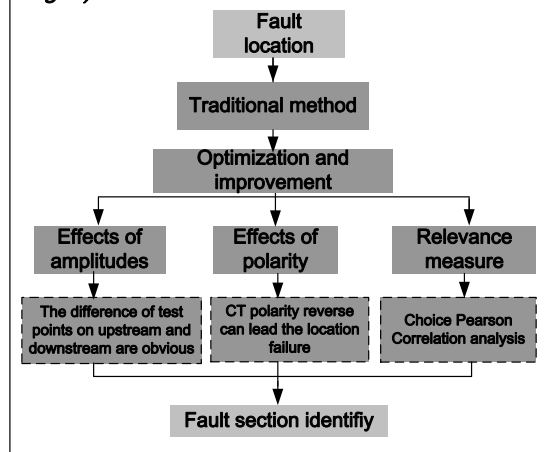
## 2 OPTIMIZATION AND IMPROVEMENT OF LOCATION METHOD

### 2.1 The principle of location method

Through the localization limitation analysis from the previous section, this paper provides comprehensive

consideration from three dimensions, as shown in figure 2.

**Fig. 2) The fault location structure**



### 2.2 The similarity measurement base on PPMCC

In the practical applications, signals acquired from CTs are often subjected to a variety of electromagnetic interference, with a certain amount of noise and zero drift. This is equivalent to adding white noise and zero drift value to the original pure fault signal. Therefore, the actual signal can be expressed as follows:

$$X = x + n(t) + \zeta \quad (4)$$

Where, X is the original pure fault signal vector; n(t) stands for the additive white noise vector;  $\zeta$  means zero drift.

In statistics, in addition to the “included angle cosine” method, Pearson Product Moment Correlation Coefficient (PPMCC/PCCs) is applied to measure the statistical indicators of the close correlation between the two sets of data.

$$p_{m,n} = \frac{\sum_{k=1}^N (x_k - \bar{X})(y_k - \bar{Y})}{\left[ \sum_{k=1}^N (x_k - \bar{X})^2 \sum_{k=1}^N (y_k - \bar{Y})^2 \right]^{\frac{1}{2}}} \quad (5)$$

Where, N represents the length of signal,  $x_k$ 、 $y_k$  stand for the kth sampling dot of the corresponding sampling signal, and  $\bar{x}$ 、 $\bar{y}$  show the average value of two signals.

PPMCC index is to comply with calculation principle of product difference method on the basis of the deviation of two different signals and their average values. The correlative degree between the two signals can be indirectly measured through two differential multiplications. When the zero drift and noise appear in the signal samples, the deviation effect causes the calculation of each sampling point to subtract the mean value and also the noise. As a result, the electromagnetic interference can be effectively suppressed, and the recognition rate of the signals can be improved.

Therefore, this paper uses PPMCC method.  $x_k$ 、 $y_k$  are equivalent to  $i_{0,m}(k)$ 、 $i_{0,n}(k)$ , the current sampling signals

of two adjacent transient zero mode currents.

### 2.3 The influence of signal amplitude on correlation

According to the section 2.1, under normal circumstances, the amplitude of the upstream zero mode current from the fault point is significantly larger than the amplitude downstream. Therefore, it is effective to use amplitude differences for measuring the correlation, which is specifically demonstrated as follows.

(1) Obtain the maximum amplitude of the transient zero mode current of each terminal device on the fault line:

$$D_{max} = \max \left( \sum_{k=1}^N i_{0,j}^2(k) \right) \quad (6)$$

Where,  $i_{0,j}(k)$  represents the zero mode current for fault line detection, j stands for the terminal number.

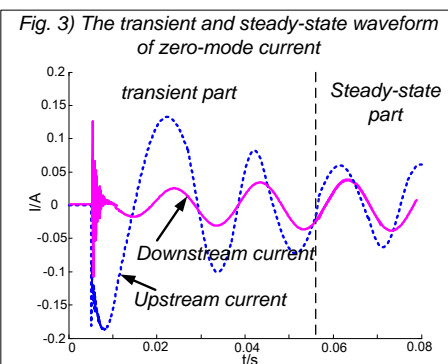
(2) Take into account the influence of amplitude correction.

$$\gamma_{m,n} = \rho_{m,n} \times e^{-\frac{1}{2} \left| \sum_{k=1}^N i_{0,m}^2(k) - \sum_{k=1}^N i_{0,n}^2(k) \right| / D_{max}} \quad (7)$$

### 2.4 Effect of CT polarity reverse connection on correlation coefficients

The traditional method does not consider the absolute value as the final criterion and ignores to improve the effective characteristic of the difference. On this basis, this paper comprehends the influence of polarity. In addition, the polarity criterion should be complied with the reference direction of both sides of CT. However, in practice there are frequent improper operations with reverse polarity or unclear polarity. The similarity of the detection terminal on both sides of the healthy section changes from positive to negative, resulting in incorrect judgment because of the polarity calculation error. Therefore, it is necessary to correct the correlation coefficient to overcome the influence of reverse polarity. The duration of fault transient state lasts for one fundamental cycle before transiting to the steady state of frequency. The free oscillation component has been attenuated during the transient time period, therefore the steady state consists mainly of the fundamental frequency. Under this situation, the influence of arc suppression coil compensation causes the currents on both sides of the fault point to have the same phase relationship, as shown in Figure 3.

Thus, when CT polarities on both sides of the fault point are in the normal states, their power frequency zero mode currents' polarities are consistent. When CT polarity is reversed, the polarity of the reversed detection point is reversed with that of non-reversed detection point. In other words, the polarity relationship of power frequency current is not related to the location of the fault point but to the normal/reversed state of the CT polarity.



Tab.2 The corresponding relation of polarity

Location type of two testing point	CT polarity	Polarity of transient current	Polarity of frequency current	Consistence of polarity relation
on one side of the fault point	normal	opposite	identical	atypism
	one point reverse	identical	opposite	atypism
	two point reverse	opposite	identical	atypism
on both sides of the fault point	normal	identical	identical	accordance
	one point reverse	opposite	opposite	accordance
	two point reverse	identical	identical	accordance

Therefore, the polarity will not be affected by reverse connection of CT through applying power frequency and transient polarity multiplication. Taking the adjacent detection point m and n as an example, the correlation coefficient after correction can be demonstrated as follows.

$$\rho_{(m,n),xz} = sign(\rho_{m,n,G}) \gamma_{m,n} \quad (8)$$

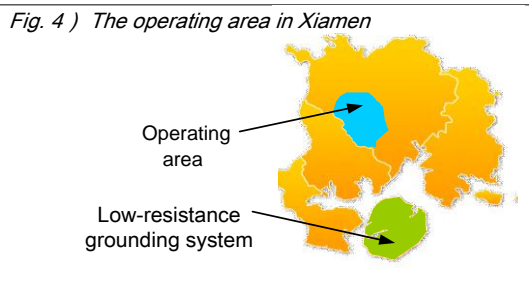
Where,  $sign(\rho_{m,n,G})$  represents the related coefficient symbol of the corresponding power current (i.e. polarity relation).

Based on the correlation coefficient, the influence of polarity relation is taken into consideration. The two detection points with opposite polarities whose correlation coefficient is greater than threshold value can be defined as the faulted section. In terms of different kinds of grounding system operating in over compensation, the polarity correction relationship is applied in order not to be affected by the reverse connection of the CT, which makes up the shortcomings of simple similarity algorithm and greatly improves the positioning accuracy.

## 3 ACTUAL SITE OPERATION

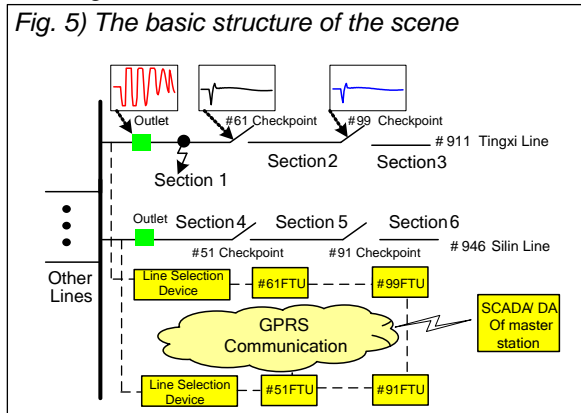
### 3.1 Brief introduction of the demonstration area

Xiamen is a city located on southeast coast of China. Its voltage level of the medium-voltage distribution system includes 35kV and below. The distribution lines are made of hybrid overhead-underground cable lines. In addition to the low-resistance grounding method used in the island, the non-solidly earthed grounding method mainly adopts isolated neutral and neutral grounding by arc extinction coils within Xiamen city, shown in figure 4.



### 3.2 Site operation analysis

In Tianyang substation with the two high-frequency routes (110kV/10kV, the neutral point grounding through arc-suppression coil), a location system for detecting non-solidly earthed fault is established, which consists mainly of three parts: a set of master station software in power dispatching centre, a line selection device in the primary substation, and distribution terminals on the line, as shown in figure 5.

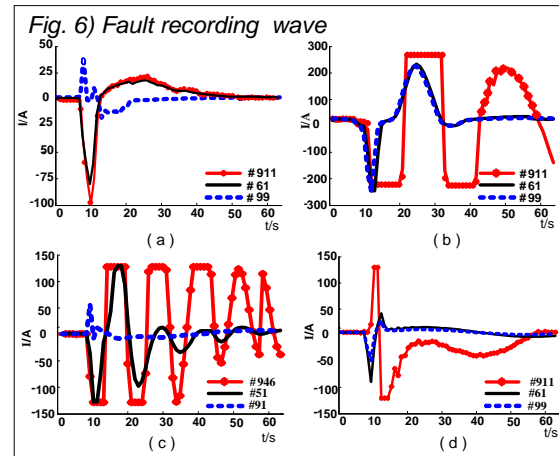


Due to space limitations, this paper only selects two sets of data as an example; the calculated results are shown in table 3 & figure 6. The sequence numbers 1 and 2 correspond to figures 6(b) and 6(d).

Sequence number 1 corresponds to the permanent grounding fault on #911 line in section 3. The zero-sequence current from line selection device has too much saturation. When using the traditional method, the influence of CT has too much saturation results in the similarity of waveform on the same side that fault point is not high. And the correlation coefficient is equal to  $|\rho_{1,2}|=0.5177<\delta$ . Therefore the sound section will be misjudged. When using the proposed method in this paper, the two correlation coefficients are greater than the setting threshold, which confirms accurately that the fault happened in the end section.

Sequence number 2 corresponds to a phase A permanent ground fault at section 1 of #911 Tingxi line. The traditional method does not consider that the polarity takes an absolute value as final value,  $|\rho_{1,2}|=0.6893<\delta$ ,  $|\rho_{2,3}|=0.9972>\delta$ . Because there is a only a small difference

between  $|\rho_{1,2}|$  and threshold value, minor deviations may cause its value to be greater than the threshold value of 0.7, resulting in wrong judgement and location failure. The corrected related coefficients comprehensively take the amplitude, polarity, threshold effects into consideration, and then calculate  $\rho_{1,2}=-0.1505<0.5$ ,  $\rho_{2,3}=0.9348>0.5$ , the difference is clearly distinguishable. Thus, it can be concluded that the fault occurs in section 1.



Tab.3 Data analysis

N.o	Type	Section 1	Section 2	Threshold	Output
1	traditional	0.5177	0.9560	0.7	Section 1
	modified	0.6684	0.9285	0.5	Section 3
2	traditional	0.6893	0.9972	0.7	Section 1
	modified	-0.1502	0.9348	0.5	Section 1

Through practical applications, the system with an accurate positioning function has recorded complete data from 17 groups of line selection devices and two FTUs, which verifies that the new method is effective and should be further promoted.

## 4 CONCLUSION

Non-solidly earthed fault has hindered the development of power supply utilities chronically. It still lacks the technology to achieve effective faulted section location. This paper focuses on the analysis and improvement of the FSL technology from the algorithm level and to make algorithm more suitable for engineering practice. The system is designed to upgrade the DA platform which is already built to avoid expensive re-development. The construction and design of line switch is simplified. Power distribution network is provided with a feasible and economical operation scheme. The system is effective to be popularized and applied.

## REFERENCES

For a book citation:

- [1] LI Tianyou, 2008, *Power Distribution Technology*, China power press, Beijing, China.

For a paper citation:

- [2] TIAN Shu, WANG Xiaowei, WANG Juanjuan, 2011, "Comparative research on fault location by transient zero—module current and transient zero-module power based on correlation analysis", *Power System Technology*. vol. 35, 206-211.
- [3] DU Gang, LIU Xun, SU Gaofeng, 2010, "Research on technology of grounding fault location combining FTU and "S" signal injecting method in distribution grid", *Power System Protection and Control*. vol. 38, 73-76.
- [4] XUE Yongduan, LI Tianyou, LI Weixin, 2014, "A Novel Method of Transient Analysis and Faulty Section Location for Single-phase Earth Fault in Non-effectively Earthed Network", *Automation of Electric Power Systems*. vol. 38, 101-107.
- [5] XUE Yongduan, XU Bingyin, LI Tianyou, 2013, "Small-current grounding fault location based on transient signals of distribution automation system", *Electric Power Automation Equipment*. vol. 33, 27-32.
- [6] SUN Bo, XU Bingying, SUN Tongjing, 2009, "A Novel Method of Transient Analysis and Faulty Section Location for Single-phase Earth Fault in Non-effectively Earthed Network ", *Automation of Electric Power Systems*. vol. 33, 83-87.

## Biography